crystals

MDPI

Review

Metal–Organic Framework Hybrid Materials and Their Applications

Joshua D. Sosa, Timothy F. Bennett, Katherine J. Nelms, Brandon M. Liu, Roberto C. Tovar and Yangyang Liu *

Department of Chemistry and Biochemistry, California State University, Los Angeles, CA 90032-8530, USA; joshdsosa@gmail.com (J.D.S.); stealmyllama@gmail.com (T.F.B.); katherinejnelms@gmail.com (K.J.N.); brandonmliu@gmail.com (B.M.L.); robtovar23@gmail.com (R.C.T.)

* Correspondence: yliu114@calstatela.edu; Tel.: +1-323-343-2323

Received: 24 July 2018; Accepted: 10 August 2018; Published: 14 August 2018

Abstract: The inherent porous nature and facile tunability of metal–organic frameworks (MOFs) make them ideal candidates for use in multiple fields. MOF hybrid materials are derived from existing MOFs hybridized with other materials or small molecules using a variety of techniques. This led to superior performance of the new materials by combining the advantages of MOF components and others. In this review, we discuss several hybridization methods for the preparation of various MOF hybrids with representative examples from the literature. These methods include covalent modifications, noncovalent modifications, and using MOFs as templates or precursors. We also review the applications of the MOF hybrids in the fields of catalysis, drug delivery, gas storage and separation, energy storage, sensing, and others.

Keywords: metal–organic frameworks; hybrid materials; post-synthetic modifications; covalent modifications; noncovalent interactions; encapsulation; layer-by-layer deposition; in situ growth; MOF (metal-organic framework) template; MOF (metal-organic framework) precursor

1. Introduction

Metal–organic frameworks (MOFs) are crystalline materials self-assembled from the coordination of polydendate ligands to metal clusters [1–3]. In addition to facile synthesis, MOF structures and properties can be uniquely tuned by customizing the metal clusters and ligands. Despite these beneficial properties, certain MOFs are hindered by physical and chemical limitations, leading to poor performance. For example, ambient moisture or high temperatures can lead to the degradation of certain MOFs' crystalline structures [4,5]. Others are limited by the high cost of precious metal nodes or expensive linkers [6], thus making mass production currently unfeasible. Additionally, some MOFs' applications are restricted by physical limitations in porosity, conductivity, or steric effects, among others [2]. Recent research has shown that hybridizing existing MOFs with external components may give rise to new materials with characteristics similar to both the parent MOF and material added. These MOF hybrid materials typically outperform their parent materials and have shown promise in the fields of catalysis [7], sustainable energy [8], gas storage and separation [9,10], drug delivery [11], detoxification [12], proton conductivity [13], energy storage [14], sensing and lighting [15,16], and supercapacitors [17], among many other fields.

Numerous methods of preparing MOF hybrids have been reported to date (Figure 1). One such method is the enhancement of MOFs through covalent modification at the metal nodes or organic ligands [18]. Covalent modification of a MOF may be used to incorporate desired characteristics of the hybridizing material within a MOF. This type of modification has been reported using metal centers of MOFs as Lewis acid sites for the attachment of external ligands or by using MOF ligands

to coordinate to other materials. In addition to covalent modifications, MOF hybrids can also be made via noncovalent interactions, such as encapsulation [19,20], layer-by-layer deposition [21], and in situ growth [22]. These methods take advantage of noncovalent interactions between MOFs and the hybridizing species by trapping the species within the MOF pores, layering them on top of the parent MOF, or growing MOFs crystals in situ with the species. Noncovalent modification allows the individual characteristics of the MOF and hybridizing materials to work synergistically in the resultant MOF hybrids while requiring less synthetic efforts than covalent modifications. These methods can be used to achieve materials with MOF coating/protection, multi-layered membranes, and the controlled growth of MOF structures with superior performance than individual parent materials. Finally, hybridizing MOFs through use as either sacrificial templates [23] or precursors [24] utilizes the ordered structure of MOFs to afford porous materials with high surface areas and uniform pore sizes. This method eliminates the metal node and/or the organic linker, leaving behind only the newly synthesized materials with the inherited uniform nanoframe of the template/precursor MOF.

In this review, we discuss each hybridization method with representative MOF hybrids from literature, as well as the hybrid materials' superior performances and applications. At the end of this review, we also summarize all reported MOF hybrid materials.

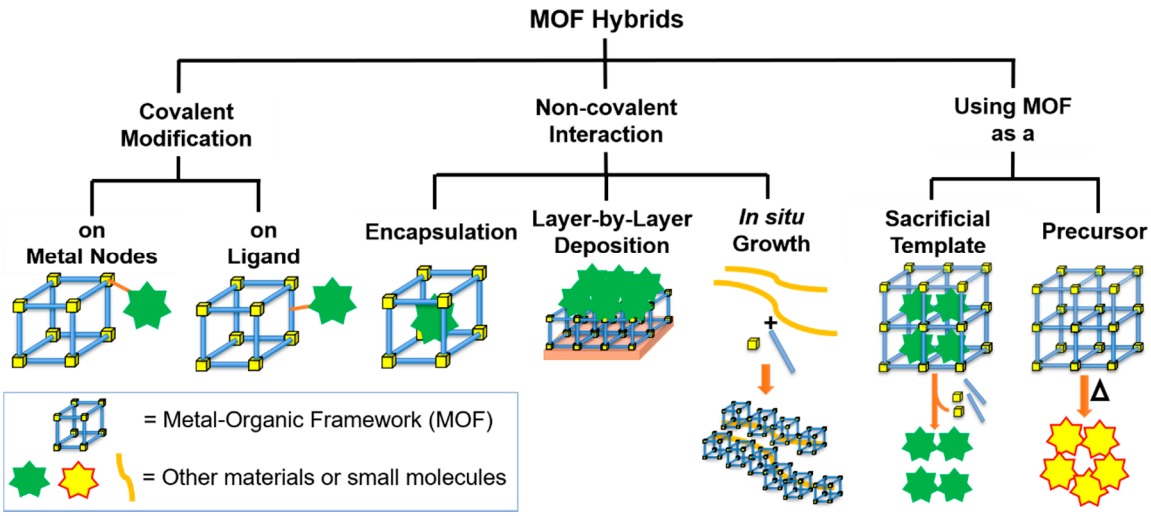

Figure 1. MOF (metal-organic framework) hybrid preparation methods discussed in this review.

2. Covalent Modifications

Covalent modifications, a subset of post-synthetic modifications (PSMs) [25], are chemical modifications of MOF lattices subsequent to synthesis, including both coordinate covalent modifications to metal clusters and covalent modifications to ligands. A variety of reactions have been explored for covalent modification of MOFs to introduce new functionality to the framework [26]. MOF structures suitable for covalent modification are generally robust and porous to avoid compromise of structural integrity. MOF hybrids have been prepared by covalently attaching other moieties to the metal nodes or ligands of MOFs. Using covalent modification, small molecules (e.g., ethylene diamine, Doxorubicin), metals/metal clusters (e.g., metal oxides, metal sulfides), and other functional materials (e.g., covalent organic frameworks (COFs), polymers, and graphene) have been hybridized with MOFs. The resultant MOF hybrids often inherit properties from both the MOFs and the materials used for covalent modification, giving rise to synergistic properties for applications in catalysis, gas storage, gas separation and drug delivery, among other fields. The notation A-B is used to represent materials A and B hybridized via covalent modification.

2.1. Covalent Modifications on the Metal Nodes

For numerous MOFs, solvent molecules in the solvation shell coordinating to terminal metal nodes can be removed and the resultant coordinatively unsaturated sites (CUSs) are exposed upon activation (i.e., desolvation by heating under vacuum) [27–29]. CUSs are available for covalent coordination with other materials, giving rise to MOF hybrids exhibiting additional and improved properties [30].

The MOF hybrid ED-MIL-101 was made by grafting electron-rich ethylene diamine (ED) to the Cr(III) nodes of the cage-structured chromium(III) terephthalate MIL-101 (Figure 2a) [31]. In this ED-MOF hybrid, the chelating amines coordinate to the Cr(III) nodes of the MOF while free amines act as Lewis base catalysts. The catalytic activity of ED-MIL-101 was evaluated via Knoevenagel condensation and determined to exhibit 91.7% conversion after 19 h. Though a slight decrease in pore size was observed, which was expected due to the addition of ED, the catalytic activity of ED-MIL-101 was greatly improved from 31.5% conversion by unhybridized MIL-101 and 74.8% conversion by APS-grafted mesoporous silica Santa Barbara Amorphous materials (SBA-15). In addition, this covalent modification was achieved with no loss of crystallinity or thermal stability of the MOF, as determined by powder X-ray diffraction (PXRD). Another ED-MOF hybrid, ED-Mg/DOBDC (DOBDC = 2,5-dioxido-1,4-benzenedicarboxylate), was prepared by covalently attaching ED to the dehydrated Mg nodes of Mg/DOBDC [32]. This hybrid exhibited enhanced capability of adsorbing and desorbing CO_2 compared to unhybridized Mg/DOBDC, as well as greater material and multicycle stability. Moreover, the hybrid structure displayed the ability to fully regenerate under mild conditions in comparison with the unhybridized MOF itself, making it more energy efficient for cyclic use.

A variety of metals and metal clusters have been covalently attached to the metal nodes of MOFs using a technique termed atomic layer deposition (ALD), resulting in MOF hybrids that exhibit unique catalytic properties [33–42]. ALD is a vapor phase deposition technique frequently used to synthesize thin films [43]. ALD in the channel-structured zirconium(IV) MOF NU-1000 has been extensively studied, owning to the MOF's mesoporous channels, high thermal stability, and -OH/-OH_2 functionalities on the Zr_6 nodes of the structure, which act as reactive sites in ALD. To date, metals (e.g., nickel ions [35]), metal oxides (e.g., zinc oxides [36,37], aluminum oxides [36,38], and indium oxides [38]) and metal sulfides (e.g., cobalt sulfide [39]) have been successfully installed on the nodes of NU-1000 using ALD (Figure 2b). The resultant MOF hybrids showed high catalytic activity for reactions such as Knoevenagel condensation [36], hydrogenation reactions [35,39], dehydration reactions [40], and water splitting [41,42]. These hybrids, M/MO_x/MS_x-NU-1000, generally showed greater catalytic activities than metal clusters alone. This is due to not only the isolated nature of metal/metal clusters on the MOF nodes, which prevents migration and agglomeration leading to improved stability, but also the high surface area of NU-1000, which can facilitate diffusion for accessibility. Remarkably, some of these hybrid catalysts obtained by ALD also exhibit high selectivity towards desired products, presumably due to the unique structures of the grafted metal/metal clusters and the confinement from the MOFs [34,40].

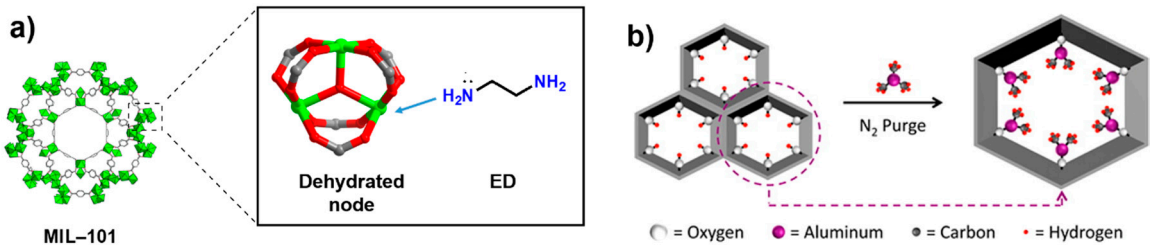

Figure 2. (**a**) The preparation of ED-MIL-101 (ED = ethylene diamine) (**b**) Using ALD (Atomic Layer Deposition) to attach AlO_x clusters on NU-1000. Figure 2b is reproduced with permission from Mondloch et al. [36]. Copyright 2013 American Chemical Society.

Fu et al. reported the preparation of COF-MOF hybrid membranes by covalently linking $Zn_2(bdc)_2(dabco)$ (where bdc = terephthalic acid and dabco = 1,4-diazabicylco[2.2.2]octane) or ZIF-8 to COF-300 membranes [44]. In both hybrids, covalent interactions between the amines of COF-300 and the Zn nodes in MOFs promote the formation of the membrane structures. Compared to individual COF and MOF materials, the COF–MOF hybrid membranes performed better in separating the H_2/CO_2 gas mixture. The [COF-300]-[$Zn_2(bdc)_2(dabco)$] and [COF-300]-[ZIF-8] exhibited separation factors of 12.6 and 13.5, respectively. Meanwhile, COF-300, $Zn_2(bdc)_2(dabco)$, and ZIF-8 membranes measured separation factors of only 6.0, 7.0, and 9.1, showing the MOF hybrid materials are significantly more selective than the individual materials and surpassing the Robeson upper-bound of polymer membranes for gas separation.

In recent years, MOF hybrids synthesized by covalent modification have also been widely studied as drug delivery systems (DDSs). In 2009, Lin et al. covalently grafted the cisplatin-based prodrug ethoxysuccinato-cisplatin (ESCP) onto amino-functionalized MIL-101(Fe) and further coated samples with a thin silica layer for stability [42]. The silica layer was then covalently grafted with the cyclic peptide c(RGDfK) to increase cytotoxicity and selectivity for the $\alpha_v\beta_3$ integrin, which is overexpressed in numerous angiogenic tumors. The resultant ESCP–MOF–silica–c(RGDfK) hybrid exhibited comparable tumor cytotoxicity (IC_{50} = 21 μM, compared to cisplatin IC_{50} = 20 μM) with additional selectivity for an angiogenic tumor integrin.

Covalent surface attachment of polymers has also been of research interest in recent years. In 2010, Férey et al. first demonstrated the potential applications of surface-attached polymers on MIL-100 and MIL-101, improving solubility [45,46]. Various MOF hybrids have since been reported for stimulus-responsive drug delivery and targeted delivery. Furthermore, pH-responsive MOF hybrid delivery systems were investigated by several groups. Wei et al. prepared a MOF hybrid by covalently attaching doxorubicin (DOX) to aldehyde-functionalized ZIF-90 via the Schiff base reaction with 13.5 wt% DOX incorporation [47]. The framework was then incorporated with the chemotherapy drug 5-fluorouracil (5-FU) with 36.35 wt% encapsulation (Figure 3a). Though DOX-ZIF-90 expressed slightly lower 5-FU loading capacity compared to the parent ZIF-90 (around 65 wt%), it is still superior over the majority of MOF loading capacities reported in literature. Additionally, pH-responsive collapse of the framework introduced faster and targeted delivery. Wei et al. were of the first to report a codelivery MOF DDS preparation by using MOF hybrids, showing MOFs' potential in combination therapy. Later, Zhang et al. and Fairen-Jimenez et al. independently studied pH-responsive MOF–PEG hybrid materials for targeted drug delivery by covalently attaching the pH-sensitive PEG polymers onto the surface of functionalized MOFs [48,49].

2.2. Covalent Modifications on the Ligands

In addition to the node modification approach, MOF hybrids can be also made by covalently attaching other materials to MOF ligands. In this case, the ligands typically have coordination sites, such as coordinatively unsaturated metals or Lewis basicity, available for further modification. This modification can be characterized by performing NMR (Nuclear Magnetic Resonance) of the acid- or base-digested MOF hybrids, revealing the organic composition of the modified ligands.

Jahan et al. prepared a graphene–MOF hybrid material by covalently attaching pyridine-functionalized graphene (reduced graphene oxide, rGO) to the metalloporphyrin centers of a Fe-porphyrin MOF [50]. Graphene sheets and graphene oxide (GO) have shown potential as an alternative to expensive precious metals (i.e., Pd and Pt) in the catalysis of hydrogen evolution (HER) and oxygen reduction (ORR) [31]. In this approach, the pyridine ligands are used to prevent aggregation of graphene and coordinate graphene to the metalloporphyrin ligands of the MOF. Catalytic studies showed that the resultant graphene–MOF hybrid has a greater selectivity for ORR than Pt-based electrodes and exhibits higher electrochemical activity, nearly ten times that of unaltered graphene. This is mainly due to the incorporation of graphene into a MOF 3D structure increasing the number of accessible active graphene sites, leading to a greater capacity of mediated

electron transfer from the larger bond polarity of the nitrogen ligand. Moreover, the well-known catalytic properties of iron-porphyrin are also improved in a MOF structure [46,51], which further improved the electrocatalytic activity of graphene. In this graphene–MOF hybrid, the rGO, pyridine ligand, and metalloporphyrin function synergistically to afford an improved catalyst compared to individual components.

Additionally, Rao et al. reported a GO-MOF hybrid membrane that was synthesized by tethering UiO-66-NH_2 onto GO surfaces, followed by incorporation into a Nafion matrix (Figure 3b) [52]. The GO surface was first coated with polydopamine (PDA) by self-polymerization. The PDA coating then formed covalent bonds with the NH_2 group on UiO-66-NH_2 via Michael addition and Schiff base reactions. The resultant GO-UiO-66-NH_2-Nafion hybrid membrane showed excellent proton conductivity in both high humidity and anhydrous conditions, which were 1.57 and 1.88 times higher than that of recast Nafion, respectively. By covalently attaching UiO-66-NH_2 onto GO, a consecutive proton transfer channel was created, resulting in the high performance of the hybrid membrane. In addition, the MOF's ability of retaining water in its pores under high humidity, as well as the acid-base pairs (-SO_3H and -NH_2) formed between Nafion and UiO-66-NH_2 under low humidity also contributed to the improved proton conductivity of the MOF hybrid. Due to the exceptional water and thermal stability of GO-UiO-66-NH_2, the hybrid membrane also had outstanding performance at high temperature and high humidity.

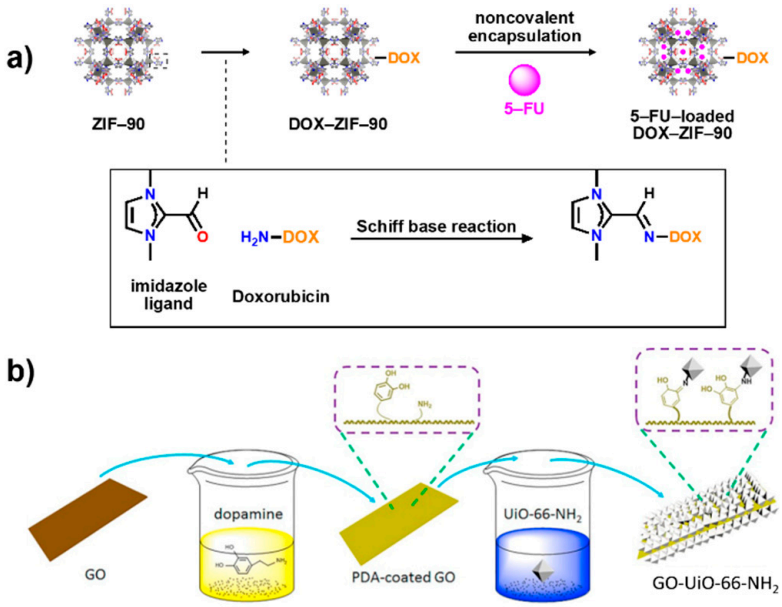

Figure 3. The preparations and structures of (**a**) DOX-ZIF-90 (**b**) GO-UiO-66-NH_2. Figure 3b is reproduced with permission from Rao et al. [52]. Copyright 2017 Elsevier.

MOF hybrids also importantly allow for biochemical selectivity of drug delivery. For example, many malignant tumors are known to overexpress folate receptors on cell surfaces, providing a potential target for selective drug delivery. Ren et al. reported the preparation of and selective drug delivery by a folate-MOF hybrid, demonstrating potential for synthetic MOF materials to interact with biochemical pathways [47]. The amine-functionalized MOF IRMOF-3 (IRMOF = isoreticular MOF, meaning MOFs with the same topology) was appended with folic acid by conjugating the IRMOF-3 amine with the folic acid carboxyl, resulting in surface amide-bound folates. Folate-IRMOF-3 was then noncovalently loaded with 5-FU, and folate conjugation was confirmed to not affect framework structure and loading capacity. Loaded IRMOF-3 (5-FU@IRMOF-3) and folate-IRMOF-3 (5-FU@folate-IRMOF-3) samples were compared for cytotoxicity in tumor lines both with and without overexpression of folate receptors. Notably, in tumor lines with overexpression of folate receptors

(KB and HeLa), treatment of 5-FU@folate-IRMOF-3 demonstrated approximately 30% lower cell viability compared to 5-FU@IRMOF-3 and 20% lower cell viability compared to free 5-FU, showing that folate-IRMOF-3 is an efficient DDS due to of folate conjugation.

3. Noncovalent Interactions

While covalent modification is a powerful tool of preparing MOF hybrids, not all materials or small molecules can be hybridized with MOFs via covalent bonding without compromise of significant functionality. In fact, many MOF hybrids have been obtained by simple mixing, coating, layering and various other methods that do not involve the formation of covalent bonds. In this section, we discuss three methods that are based on noncovalent interactions: encapsulation, layer-by-layer deposition, and in situ growth. It should be noted we only discuss three methods here as examples, but there are various other methods reported that are based on noncovalent interactions.

3.1. Encapsulation

In this review, "encapsulation" denotes the process of introducing other materials within existing MOF pores without directly bonding to the MOF structures. The notation A@B is used to represent material A encapsulated in material B. To date, a variety of materials have been encapsulated into MOFs to produce MOF hybrids that are more stable and superior, often with new functionality. The successful encapsulation of materials inside MOF pores is typically characterized by transmission electron microscopy (TEM), UV-Vis spectroscopy, and/or NMR spectroscopy.

Encapsulation of noble metal nanoparticles (NPs) in MOFs, most commonly Pt and Pd NPs, has enhanced their stability as well as catalytic performance [19,53]. Successful encapsulation of NPs into MOF crystals has been achieved by incorporating NPs during solvothermal MOF synthesis [19]. This process does not affect the crystallinity of MOFs, and it allows for controlled distribution of NPs as well as the inclusion of multiple types of NPs within one MOF [54]. For example, Pt@UiO-66 obtained using this method exhibited reactant shape selectivity (RSS) in olefin oxidation due to the MOF confinement, which only allow smaller substrates that are able to diffuse through UiO-66 pores to react. In comparison, the non-encapsulated Pt NPs showed no selectivity towards different substrates, and UiO-66, the MOF alone, did not exhibit catalytic activity. In addition to contributing RSS to the NP@MOF hybrids, MOFs can also prevent the aggregation of encapsulated NPs, thus further enhancing their catalytic activity through increased surface area. Another core-shell hybrid, Pd@IRMOF-3, exhibited a greater catalytic activity than either parent material, as well a greater performance over IRMOF-3-supported Pd; this hybrid showed promise in cascade reactions to produce 2-(4-aminobenzylidene)-malononitrile, where the IRMOF-3 shell was used for Knoevenagel condensation followed by selective hydrogenation via Pd NP cores [55]. Encapsulation of non-noble metal NPs within MOFs have also been reported; one such hybrid is Cu(I)@MOF-5, which exhibited enhanced ability of separating dibenzothiophene (DBT) from crude oils. A spontaneous monolayer dispersion technique was employed to reach the dispersion threshold of the ions within the MOF-5 network, which increased the adsorption and desorption of thiophenic sulfur compounds at a low cost of production [56].

MOFs have also been studied for the encapsulation of polyoxometalates (POMs). POMs are a class of polyatomic materials consisting of linked metal oxyanions, similar to some MOF metal clusters, that are useful for redox catalysis but limited in activity by their low surface area and poor stability. Many studies have employed MOF encapsulation of POMs to overcome these limitations, increasing surface area [57] and distribution of catalytic material [58] while also preventing aggregation [59]. Furthermore, POM@MOF hybrids frequently demonstrate greater catalytic activity than either POM or MOF parent material. In one such study, Buru et al. encapsulated the POM $H_3PW_{12}O_{40}$ into NU-1000 by suspending NU-1000 in an aqueous solution of $H_3PW_{12}O_{40}$ [15]. The resultant hybrid material, PW_{12}@NU-1000 (Figure 4a), showed good stability towards leaching in aqueous solution, as the nodes of NU-1000 act as counterions for $[PW_{12}O_{40}]^{3-}$. Subsequently, PW_{12}@NU-1000 was used as

a catalyst for sulfide oxidation in the presence of hydrogen peroxide as both the POM and Zr_6 nodes of NU-1000 catalyze the sulfide oxidations. A similar study conducted by Zou et al. encapsulated POMs within a metalloporphyrin-based MOF via stepwise reactions between POM ($H_3PW_{12}O_{40}$) and MOF precursors (first with Mn^{III}Cl-tetrapyridylporphyrin, then with $Cd(NO_3)_2 \cdot 4H_2O$). As such, this hybrid demonstrated the combined catalytic effects of the Mn-porphyrinic ligand and the encapsulated POM, thus acting as a powerful heterogeneous catalyst [60].

A perovskite quantum dots (QDs) encapsulated MOF was prepared by introducing the QDs precursors (PbI_2 and CH_3NH_3X, X = Cl, Br, and I) into an oriented microporous MOF HKUST-1 (a MOF named after Hong Kong University of Science and Technology) by immersing the MOF thin films in the precursor solutions (Figure 4b) [16]. The resultant QDs exhibited uniform ultrasmall particle size (1.5–2 nm), which matches the pore size of HKUST-1. In this case, HKUST-1 not only serves as the scaffold that controls the particle size of the $MAPbI_2X$ QDs, it also protects the encapsulated QDs from moisture. The hybrid $MAPbI_2X$@HKUST-1 exhibited excellent stability in moist air (70% humidity), while the $MAPbI_2X$ decomposed under the same condition. Additionally, these QD@MOF hybrids also had longer luminescent lifetimes compared to perovskite $MAPbI_2X$, with the longest lifetime occurring when X = Br in the MOF hybrid material.

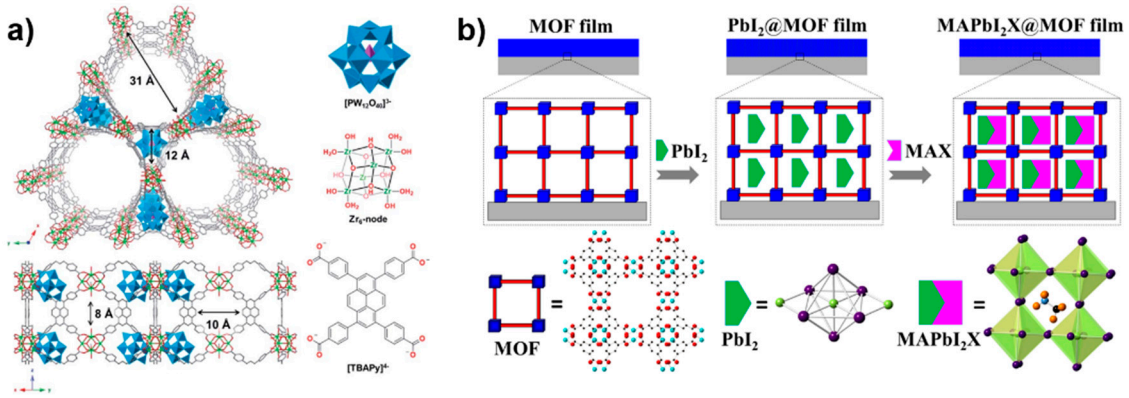

Figure 4. (**a**) The structure of PW_{12}@NU-1000. (**b**) The preparation of $MAPbI_2X$@HKUST-1. Reproduced with permission from Buru et al. [58] (Copyright 2018 Royal Society of Chemistry) and Chen et al. [16] (Copyright 2016 American Chemical Society), respectively.

The encapsulation of gold nanoclusters (AuNC) in ZIF-8 yielded a hybrid material capable of selectively sensing H_2S in liquid and gas phases [61]. The synthesis of the hybrid AuNC@ZIF-8 was achieved through the introduction of the MOF metal source, $Zn(NO_3)_2$, into a AuNC solution of pH ranges 3.8–6.2. It was found that at a pH of 5, the zinc ion demonstrated its highest coordination ability, resulting in increased precipitate. AuNC@ZIF-8 was obtained when the precipitate was placed into a solution of 2-methylimidazole. It was determined that the encapsulation was not possible when ZIF-8 was synthesized directly followed by the introduction of an AuNC solution. The quantum yields and lifetimes of AuNC were found to significantly improve through their interactions with ZIF-8, increasing from 7.6% and 2.96 μs to 33.6% and 9.18 μs. Furthermore, based on the reductive tendencies of H_2S and the affinity of gold for sulfur, the increased luminescent properties of AuNC@ZIF-8 were effectively quenched in the presence of Na_2S in solution, with a detection limit of 0.54 μM. Gas phase studies of H_2S revealed similar selectivity and sensitivity. In addition, similarly encapsulated MOFs are also being studied for the sensing of H_2 [62], various anions [63], and Cu^{2+} ions [64].

With the intention of yielding a material appropriate for visible-light communication (VLC), Wang et al. encapsulated rhodamine B (a yellow light emitter) inside of an Al-based MOF with the 9,10-bis(*p*-benzoic acid)anthracene (DBA) linker (blue light emitter), obtaining a white light emitter [65]. Currently, the limited speed of VLC is attributed to the use of materials with long lifetimes, around

200 ns, that results in a low intrinsic modulation frequency. The use of organic dyes, such as rhodamine B, are believed to be a potential solution to this, as they could provide lifetimes as short as 1 ns while maintaining high quantum yields. However, quenching induced by solid state aggregation of organic dyes make them unideal candidates. Therefore, the encapsulation of rhodamine B in a MOF was analyzed as a potential solution to prevent aggregation and produce a white light source through the appropriate selection of a blue light emitting linker. It was found that the interactions between the excited linker and encapsulated molecules provided a bridge for energy transfer that would combine the effect of blue and yellow emission to create various hues of white light. The results indicated that depending on the concentration of rhodamine B encapsulated in the MOF, the desired white light emission could be obtained. A 0.019% rhodamine B encapsulated MOF, RhB-0.019%@Al-DBA, gave the best results, with 6085 K white light color temperature, a lifetime of 5.4 ns, and a corresponding intrinsic modulation frequency increase to 3.6 MHz from 0.8 MHz.

3.2. Layer-by-Layer Deposition

Synthesis of MOF hybrids through deposition often involves the formation of membrane-based material by depositing layers of MOFs and other materials. Deposition is similar to encapsulation in that other materials can adhere to the surface of a MOF and in that the elements incorporated can be customized per application. It is worth noting that the "Layer-by-Layer Deposition" section discussed in this review only includes examples of MOF hybrids based on noncovalent modifications. Covalent bonds can exist in MOF hybrid materials made using this method but are not as common, so we include relevant examples in the "Covalent Modification" section (hybrids made from ALD and COF-MOF hybrids). Using this technique, metal clusters, metal oxides, graphene oxide, and polymers have been hybridized with MOFs, giving rise to new materials that are useful in gas separation, catalysis, photovoltaics, and proton conducting [52,53,56,66–69]. The notation A | B | C is used to represent materials A, B, and C that are hybridized via layer-layer deposition.

MOF membranes have been extensively studied for various separation processes. Combining the properties of MOFs and other materials, MOF hybrid membranes often exhibit superior performance than membranes based on individual materials [70–72]. For example, a MOF-polymer hybrid membrane synthesized by Bae et al. showed high performance for CO_2/CH_4 separation and great gas permeability [70]. This hybrid membrane was made by incorporating submicrometer-sized (0.81 ± 0.05 μm) ZIF-90 crystals onto a 6FDA-DAM poly(imide) and its performance was evaluated under mixed-gas conditions (1:1 CO_2/CH_4 mixture at 25 °C and 2 atm total feed pressure). ZIF-8 | 6FDA-DAM hybrid membrane with 15 wt% ZIF-8 showed CO_2 permeability of 720 Barrer and CO_2/CH_4 selectivity of 37, while these values were 390 Barrer and 24, respectively, for pure 6FDA-DAM (Figure 5a).

In addition to gas separation, MOF hybrid membranes have also offered new opportunities for catalysis. Pd clusters were deposited onto Zn/Ni-MOF-2 nanosheets to form hybrid membrane, Pd | Zn/Ni-MOF-2, that exhibited greater catalytic activity towards CO-based reactions (alkoxycarbonylation of aryl halides) than the individual Zn/Ni-MOF-2 sheets and Pd clusters, as well as TiO_2 immobilized Pd clusters [73]. The better catalytic performance of the Pd | Zn/Ni-MOF-2 hybrid membrane over others was believed to be attributed to the porous MOF nanosheets that can adsorb CO into the hybrid membrane. In another study by Maina et al., ZIF-8 membrane doped with semiconductor nanoparticles, TiO_2 and $CuTiO_2$, were deposited on a ZIF-8 | GO hybrid membrane [53]. Compared to unmodified ZIF-8, the resultant fabricated membrane $CuTiO_2$ | ZIF-8 | GO showed higher photocatalytic efficiency toward CO_2 conversion, producing 70% more methanol with 7 μg of doped $CuTiO_2$. In addition to high CO_2 adsorption capacity of the MOF (ZIF-8), the MOF structure also provided a kinetic route to transport the photogenerated electrons by semiconductor nanoparticles to CO_2 [74]. Both factors contributed to the enhanced catalytic activity of the hybrid membrane.

More recently, MOF hybrid membranes were found useful in solar energy harvesting and conversion [52,66,69]. Lee et al. prepared a TiO_2 | nanotube | MOF hybrid membrane that showed

enhanced photovoltaic performance [66]. A composite film containing TiO_2 nanoparticles and multi-walled carbon nanotubes was first synthesized hydrothermally. It was then sensitized with Cu-based MOFs (copper(II) benzene-1,3,5-tricarboxylate) via layer-by-layer deposition [75]. Combining the nanotube's ability of accelerating electron transfer and the small charge transfer resistance after MOF sensitization, the resultant hybrid membrane showed an increase of nearly 60% in power conversion efficiency in comparison to the unmodified MOF cell [76].

3.3. In Situ Growth

In situ growth approach involves the growth of MOF crystals via solvothermal/hydrothermal reactions of the metal salts and ligands in the presence of another material. During the synthesis, the second material generally serves as a structure directing agent, leading to oriented growth of MOF crystals [77,78]. Hybrid materials obtained by in situ growth approach usually have ordered morphology and/or hierarchical structure, which are useful features for applications such as gas storage and small molecule separations [17,79–81]. In this section, a MOF that is grown in situ on another material A is denoted as MOF@A.

In a study by Chen et al., HKUST-1 was synthesized in the presence of SBA-15 by adding a small amount of SBA-15 with MOF precursors to form HKUST-1@SBA-15 (Figure 5b) [82]. The carbon structures are integrated into the hybrid material and serve as a template for HKUST-1 to grow. Silanol groups from SBA-15 and the metal centers in HKUST-1 interact, inducing the formation of new mesopores as well as an increase of surface area and micropore volume. Furthermore, the formation of the MOF composite on SBA-15 reduced the crystal size of the hybrid structure, which controlled the morphology and attained a more ordered structure. From the various concentrations of SBA-15 to MOF ratio, the hybrid synthesized from a 1 wt% SBA-15 solution produced the greatest increase in CO_2 adsorption, by 15.9% compared to HKUST-1.

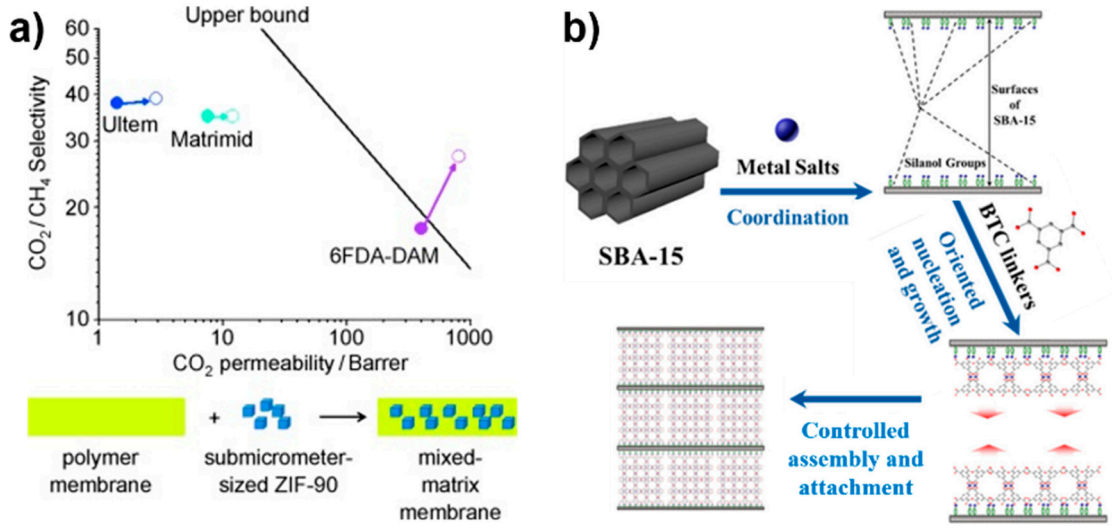

Figure 5. (**a**) MOF-polymer hybrid membranes prepared by lay-by-layer deposition and their enhanced performances. (**b**) The in situ growth of HKUST-1 on SBA-15. Reproduced with permission from Bae et al. [70] (Copyright 2010 John Wiley and Sons) and Chen et al. [82] (Copyright 2017 American Chemical Society), respectively.

Zheng et al. prepared a MOF hybrid by the in situ growth of IRMOF-3 on stainless steel wires [80]. This hybrid was further coated by ionic liquid (IL, [bmim] [PF_6]) and polymethylsioxane (PDMS) to improve its moisture and thermal stability. The resultant IRMOF-3@ILs/PDMS hybrid material not only showed a dramatic increase in resistance to high temperature and moisture, as well as an increase of 100 times the lifespan of the original ILs, but also a much better extraction

efficiency for selected polycyclic aromatic hydrocarbons (PAHs) compared to each individual material. The improved extraction efficiency of the MOF hybrid was due to the π–π interactions between PAHs and IRMOF-3, [bmim] [PF_6], as well as the larger surface area of IRMOF-3 that resulted from the in situ growth method.

Falcaro et al. prepared MOF-5 crystals by adding a surfactant (Pluronic F-127) into traditional solvothermal synthesis process [83]. The reaction between the surfactant and Zn^{2+} in solution produced poly-hydrate zinc phosphate microparticles that act as nucleation seeds in MOF synthesis, which accelerated the growth of the MOF into either single crystals or multifaceted crystals surrounding the microparticles. Functional MOF hybrids can be directly prepared by introducing functional nanoparticles into these nucleation seeds (poly-hydrate zinc phosphate microparticles). In these MOF hybrids, it was found that the functional nanoparticles were evenly distributed throughout the interior of the MOF as opposed to its external surface. This method offers greater spatial control over the distribution of the interested functional species in MOFs when compared to other methods such as ALD, deposition, or encapsulation. Using this method, MOF-5 doped with various functional nanoparticles (e.g., metals, QDs, polymers) were prepared, and the resultant QDs@MOF-5 hybrids were used as selective molecular sieve sensors. In addition, this method was found to be 70% faster than traditional solvothermal methods, showing that using surfactants is a promising in situ growth approach for MOF hybrid synthesis.

4. Using MOFs as Sacrificial Templates or Precursors

The use of MOFs as sacrificial templates or precursors is a rising field of study as several key properties of MOFs provide numerous benefits over previous technology; most notably, the tunable nature of MOFs allows for versatile and customizable templates/precursors, and the uniform distribution of the ligand and metal nodes within MOFs often leads to a uniform distribution of the resulting hybrid material [1]. It has been shown that the hybrid materials produced by sacrificial MOFs share comparable structures and pore sizes to their parent MOFs., especially those produced through carbonization [2]. Carbonization, calcination, pyrolysis and annealing are the common methods of preparing materials using MOFs as sacrificial templates/precursors. Another advantage of using MOFs as templates/precursors is that their organic components can be used to produce carbon materials via combustion synthesis without external carbon sources in a single step [2,3]. Alternatively, the ligands of the template/precursor MOFs can also be removed by high temperature or acid treatment, leaving the metal clusters or metal oxides with high surface areas. Essentially, MOF template/precursor method allows for the facile synthesis of porous carbon nanomaterials, highly dispersed metal clusters and porous metal oxides. Materials produced through this method are promising as environmentally benign and cost-efficient solutions for energy storage [4]. In particular, they can be applied to supercapacitors as electrode or anode materials [3–5], fuel cells [2], and semiconductors [2]. In addition to these, some of them are also useful in catalysis [5] and sensing [84].

4.1. MOFs as Sacrificial Templates

In the process of material preparation, if the MOF framework was used as a structural pattern for the synthesis of the new material, and both metal nodes and ligands of the MOF were removed or decomposed afterwards, we categorize this method as "using MOFs as sacrificial templates". Typically, the MOF templates can be completely removed by either high temperature or acid treatment.

In 2008, Liu et al. for the first time used a MOF as a sacrificial template to synthesize porous carbon, via the carbonization of a polymer/MOF hybrid (furfuryl alcohol polymerized in MOF-5 pores) [3]. After carbonization at 1000 °C, the framework of MOF-5 completely decomposes and served as a self-sacrificed structural template, resulting in a carbon material with high surface area and pore sizes ranging from micro- to macropores, evidenced by N_2 sorption isotherms. The introduction of furfuryl alcohol into the cages of the MOF structure serves as an outside carbon source. At −196 °C and 760 Torr, the resultant porous carbon material adsorbed more hydrogen gas than MOF-5.

In addition, the meso/macropores of the obtained porous carbon, resulting from the sacrificial MOF template, endow it with exceptional electrochemical properties that are ideal for using as electrode material. It had better performance than other carbon materials such as SBA-15 derived carbons [11]. Later on, Jeon et al. used nitrogen-containing IRMOF-3 as a sacrificial template, without any additional carbon sources, to synthesize nitrogen-doped porous carbon to be used as supercapacitors [81]. The MOFs were prepared solvothermally, followed by carbonization under argon gas at varying temperatures, ranging from 600–950 °C, to determine which temperature produced the purist compound. At carbonization temperatures of 950 °C, the nitrogen-doped porous carbon had a capacitance of 239 F g^{-1}. By comparison, analogous nitrogen-free carbon had a capacitance of 24 F g^{-1}. This shows that the nitrogen dopants provided by the organic linkers of the MOF was the cause of the increased capacitance. Chaikittisilp et al. also synthesized nanoporous carbon for supercapacitor applications by utilizing ZIF-8 as the sacrificial template [85]. The porous nature and high surface area of ZIF-8 made it an ideal template for preparing porous carbons through carbonization, with results showing the relationship between carbonization temperatures and BET surface areas of the obtained porous carbons (carbonization temperatures of 600 to 1000 °C resulted in surface areas of 520 to 1110 m^2 g^{-1}).

Recently, Yang et al. prepared hollow and highly porous titania and other composite materials by using ZIF nanocrystals as sacrificial templates as shown in Figure 6a [86]. A core-shell structured composite ZIF@TiO_2 was first obtained by heating $Ti(OBu)_4$ in the presence of ZIF (ZIF-8 and ZIF-67) nanocrystals. The ZIF core of the composite was then completely removed by the addition of dilute aqueous HCl solution, producing the hollow amorphous TiO_2. They also found that by using ZIF cores of varying shapes and dimension, the morphologies and particle sizes of the resultant hollow amorphous TiO_2 can be controlled. 77 K N_2 adsorption experiments showed that the hollow TiO_2 materials had surface areas comparable to their ZIF templates. Owning to their high surface areas, along with great chemical and thermal stability, the hollow TiO_2 materials made from ZIF templates are excellent catalyst supports. To utilize the TiO_2 as catalyst support, ZIF-8 infused with Pt NPs was used as the template for TiO_2 synthesis, resulting in Pt/ZIF-8@TiO_2 core-shell structure. Using the same acid etching method, ZIF-8 template was completely removed and resulted in Pt NP encapsulated hollow TiO_2, Pt@TiO_2. Having isolated and well-dispersed Pt NPs encapsulated in a robust and porous TiO_2, the Pt@TiO_2 prepared using MOF templating method is an excellent catalyst for hydrogenation reactions.

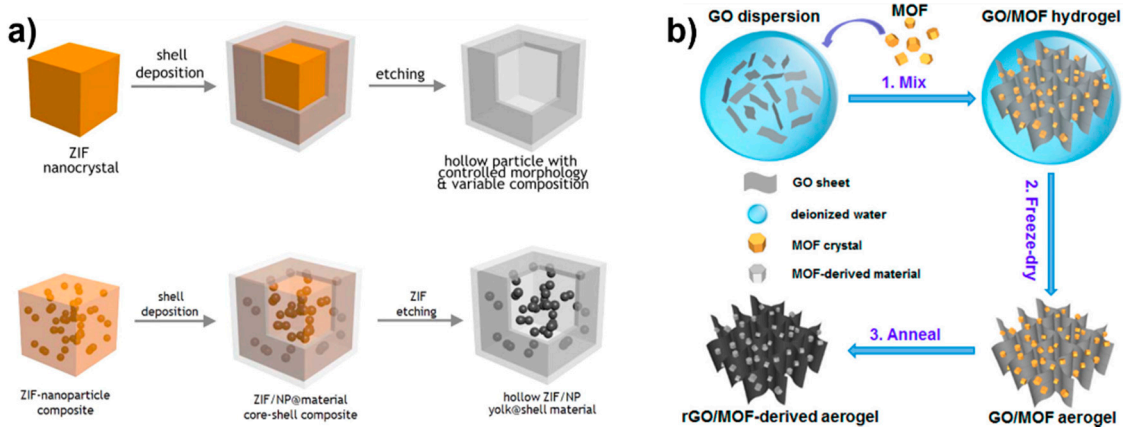

Figure 6. The preparations and structures of (**a**) ZIF@TiO_2 and Pt/ZIF-8@TiO_2, and (**b**) MOF-derived rGO/Fe_2O_3. Reproduced with permission from Yang et al. [86] (Copyright 2015 American Chemical Society) and Xu et al. [87] (Copyright 2017 American Chemical Society), respectively.

4.2. MOFs as Sacrificial Precursors

If parts of the MOF components, usually metal nodes, remain after the process either in the original metal cluster or transformed metal oxide forms, we categorize this as "using MOFs as sacrificial precursor." In most cases, when using MOF as a precursor, the 3D structure simultaneously works as template in synthesis.

Malonzo et al. used NU-1000 as a sacrificial template and precursor to produce a thermally stable catalyst with high concentration of single catalytic sites that were derived from the metal clusters of the MOF [88]. In the catalyst preparation, a silica layer was first created inside the MOF channels by the polycondensation of tetramethylorthosilicate. The composite was then heated 500 °C in air to remove the organic linkers of NU-1000, leaving the Lewis acidic oxozirconium clusters of the MOF anchored in the silica layer while retaining the MOF's uniform 3D channel structure (3 nm). Pyridine adsorption experiments and a glucose isomerization reaction demonstrated that the oxozirconium clusters in this catalyst remained accessible and catalytically active after heating to 600 °C in air, while the metal clusters in pristine NU-1000 aggregated and transformed to ZrO_2 nanoparticles under the same condition. In another study, a Cu-based MOF HKUST-1 was used as the sacrificial precursor, which underwent thermolysis followed by carbonization, to produce CuNPs@C [89]. This hybrid material showed catalytic ability that mimics horseradish peroxidase (HRP), which can catalyze the oxidation of 3,3′,5,5′-tetramethylbenzidine (TMB) in the presence of hydrogen peroxide. Compared to HRP, this hybrid prepared from HKUST-1 precursor is not only more stable and less expensive, but also showed a higher affinity for hydrogen peroxide, resulting in its higher catalytic activity. A colorimetric method was developed using CuNPs@C for the detection of ascorbic acid with higher sensitivity than that based on HRP.

Xu et al. used a 3D graphene oxide/MOF composite as a precursor to produce a MOF-derived 3D composite aerogel, rGO/Fe_2O_3 [87]. As shown in Figure 6b, this aerogel was prepared by first forming a GO/MOF hydrogel through adding MOF crystals into an GO aqueous solution, followed by freeze-dry and a two-step annealing process. During the two-step annealing process, GO was reduced to rGO and Fe-MOFs transformed to Fe_2O_3, while the porous structure of the aerogel is maintained. Owing to the 3D porous structure of the Fe-MOF precursor, the resultant Fe_2O_3 nanoparticles formed porous nanostructures. This Fe_2O_3 porous nanostructures with high active surface area, along with the 3D well-defined graphene with large electric double-layer capacitance, are ideal electrode materials for energy storage devices. Experiments showed that electrodes built from the hybrid rGO/Fe_2O_3 performs better than electrodes of only rGO or Fe_2O_3. Xu et al. also utilized this hybrid rGO/Fe_2O_3 as electrode materials to construct a flexible all-solid-state supercapacitor device, which exhibited a high volumetric capacitance (250 mF cm^{-3} at 6.4 mA cm^{-3}) and a great capacitance retention (96.3% after 5000 cycles at 50.4 mA cm^{-3}).

Using Fe (Fe^{3+})-doped MOF-5 as a sacrificial template and precursor, Song et al. developed a hollow nanocage transition-metal oxide (TMO) semiconductor with the intention of selectively sensing acetone [84]. Fe-doped MOF-5 underwent an annealing process to afford $ZnFe_2O_4$ hollow concave octahedral structure. The synthesis of such a complex multimetal TMO is facilitated by the Zn and Fe composition of the doped MOF, resulting in a stable structure that could be annealed in air. The use of $ZnFe_2O_4$ is well researched as a fruitful semiconductor material, and the high specific surface area as well as the porous nanostructure of the TMO derived from the doped MOF precursor led to greater stability and better performance compared to $ZnFe_2O_4$ being prepared with other methods. Ultimately, $ZeFe_2O_4$ prepared from the sacrificial MOF precursor showed exceptional sensitivity for acetone at a concentration range of 64.4–200 ppm, optimally at 120 °C. It also exhibited good selectivity and cyclic stability.

In addition to the MOF hybrids discussed in each section, we also summarize and categorize all reported MOF hybrids in Table 1 based on their preparation methods.

Table 1. A summary of reported MOF hybrids and their applications.

Hybrid Method		MOF Used	Hybridized with	Applications	Ref
Covalent Modification	on metal nodes	Cr(III) MIL-101	Ethylene diamine	Catalysis	[90]
		Mg/DOBDC	Ethylene diamine	Gas storage	[32]
		NU-1000	ALD in MOFs: Ni, ZnO_x, AlO_x, InO_x, CoO_x, CoS_x, Cu_2O, $Ca(OH)_2$, SiO_2, HfO, WO_x, PtO	Catalysis	[37,39–41,91–96]
		UiO-66	ALD in MOFs: Ni; 4-(azidomethyl)benzoic acid, then PEG alkyne	Catalysis; drug delivery	[35,49]
		$Zn_2(BDC)_2(DABCO)$ and ZIF-8	COF-300 (SiO_2 and polyaniline disks)	Gas separation	[44]
		MIL-88A and MIL-100	CH_3-O-PEG-NH_2	Drug delivery	[45]
	on ligands	UMCM-1-NH_2	$[Fe(acac)_3]$ and $[Cu(acac)_2]$	Catalysis	[97]
		Zr-MOF-bpy	$CuBr_2$	Catalysis	[98]
		$(Fe-P)_n$ MOF	pyridine functionalized rGO sheets	Catalysis	[50]
		IRMOF-3	vanadium clusters, Folate	Catalysis, drug delivery	[47,99]
		MOF-253	Rhenium, Rubidium	Catalysis	[100]
		MIL-101(Fe)-NH_2	Ethoxysuccinato-cisplatin, then thin silica coating	Drug delivery	[42]
		ZIF-90	Doxorubicin	Drug delivery	[47]
		MIL-101(Fe)-N_3	Bicyclonyne-functionalized β-CD, then PEG-Ad	Drug delivery	[41]
Non-covalent Interactions	Encapsulation	UiO-66	Pt NPs, Pd NPs	Catalysis	[19,101]
		IRMOF-3	Pd NPs	Catalysis	[55]
		$[Cd(DMF)_2Mn^{III}(DMF)_2TPyP]_n^{3n+}$	POMs	Catalysis	[60]
		NU-1000	POMs	Catalysis	[15,58]
		MIL-100(Cr)	POM-MIL-100(Cr) with Ru NPs	Catalysis	[58]
		Ni-PYI	Ni NP-supported POMs	Catalysis	[102]
		HKUST-1	quantum dots (QDs)	Photovoltaics	[16]
		ZIF-8	Branched poly-(ethylenimine)-capped carbon QDs; ZnO; Au, Ag, NaYF4, Pt and CdTe NPs	Sensing, catalysis	[54,61,62,64]
		Rho-ZMOF	Pt-metalated porphyrin	Sensing	[63]
		Eu-MOF	CdTe QDs	Photovoltaics	[103]

Table 1. *Cont.*

Hybrid Method		MOF Used	Hybridized with	Applications	Ref
		MIL-101	H_2SO_4, Toluenesulfonic, triflic acids	Proton conductivity	[13,84]
		Zn-NPD	Naphthalene	Sensing	[104]
		Al-DBA	Rhodamine B	Lighting	[65]
		Zn-DPP	Co-doped Tb^{3+} and Eu^{3+}	Lighting	[105]
	Layer-by-Layer Deposition	ZIF-8	$TiO_2/Cu-TiO_2$ and GO	Catalysis	[53]
		Ti-MOF	Pt NPs	Catalysis	[67]
		MIL-100(Fe)	Phosphated β-CD, then PEG-Ad	Drug Delivery	[68]
		HKUST-1	TiO_2 and multi-walled carbon nanotubes	Photovoltaics	[66]
		UiO-66	GO	Proton conductivity	[52]
		UiO-66-SO_3H	GO nanosheets	Proton conductivity	[69]
		MOF-5	Cu(I)	Desulfurization of flue gas	[56]
	In situ Growth	Cu-TED-BDC	GO sheets	Catalysis	[106]
		ZIF-8	Polysulfone, Matrimid	Gas separation	[71]
		MOF-5	Multi-Walled Carbon Nanotubes, Pt-loaded Multi-Walled Carbon Nanotubes, Polymeric Ionic Liquids, Matrimid, Pluronic F127	Gas storage, gas separation, PAHs extraction, sensing	[72,80,83,107–109]
		HKUST-1	Pt-loaded GO, SBA-15, Li-Doped Carbon Nanotubes, Matrimid	Gas storage, gas separation	[71,82,110,111]
		UiO-66-NH_2	Polysulfone	Gas separation	[112]
		ZIF-90	Ultim, Matrimid, 6FDA-DAM	Gas separation	[70]
		MIL-53(Al)	Matrimid	Gas separation	[71]
		MOF-74(Zn)	Alginate	Molecular sieves	[78]
Using MOF as a	Template	$Fe_3[Co(CN)_6]_2$	Graphene	Catalysis	[113]
		MIL-88 (Fe)	carbon-film-coated iron sulfide nanorods (C@Fe_7S_8)	Li ion battery	[14]
		MOF-5	Nitrogen-doped porous carbon; Carbon	Supercapacitors; electrodes; catalyst support	[81,114]
		ZIF-67	Ni-Co layered double hydroxides on graphene nanosheets, $Ti(OBu)_4$	energy storage, catalyst support	[86,115]

Table 1. *Cont.*

Hybrid Method	MOF Used	Hybridized with	Applications	Ref
	ZIF-8	Nanoporous carbons, $Ti(OBu)_4$	Electrode materials, fuel cells, supercapacitors, catalyst support	[85,86,89]
	HKUST-1	Mo-POMs	Energy storage, electronics, sensing and catalysis	[85,116]
Precursor	HKUST-1	Decomposition of the organic MOF ligand into a Cu-supported carbon matrix	catalysis	[89,117]
	NU-1000	Nanocasting with silica	catalysis	[88]
	Co-NDC	Carbonization of Co-NDC grown on Cu sheets	Catalysis	[118]
	MOF-5	Zn/Ni-MOF-5 to MOF-2 nanosheets followed by deposition of Pd clusters	catalysis	[73]
	MIL-53 (Fe)	porous Fe_2O_3 nanostructures	Li ion battery	[24,73]
	$[Co_3L_2(TPT)_2xG]_n$	Porous Co_3O_4 hollow tetrahedra	Li ion battery	[119]
	MOF-200	Nitrogen-doped graphene wrapped okra-like SnO_2 composites	Li ion battery	[120]
	$[Co(BIB)(o\text{-}BDC)]_\infty$, $[Co_2(BIB)_2(m\text{-}BDC)_2]_\infty$, and $\{[Co(BIB)(p\text{-}BDC)(H_2O)](H_2O)_{0.5}\}_\infty$	Porous Co@carbon nanotube composites (CO@CNTs) and after in situ gas-sulfurization (CoS_2@CNTs)	Supercapacitor	[121]
	Fe-MOF, Ni-MOF, ZIF-8, MOF-5, Sn-MOF, Co-MOF	Graphene oxide composite aerogels: rGO/Fe_2O_3 and rGO/NiO/Ni	Supercapacitor	

Abbreviations: DOBDC = 2,5-dioxido-1,4-benzenedicarboxylate, BDC = 1,4-benzenedicarboxylic acid, DABCO = 1,4-diazabicyclo[2.2.2] octane, acac = acetylacetonate, bpy = bipyridine, ad = Lys(adamantane)-Arg-Gly-Asp-Ser-bi-PEG1900 (bi = benzoic imine bond), TPyP = tetrapyridylporphyrin, PYI = L- or D-pyrrolidin-2-ylimidazole, NPD = naphthalene diimide, DBA = 9,10-dibenzoate anthracene, DPP = 1,3Di(4-pyridyl)propane, TED = triethylene diamine, NDC = naphthalenedicarboxylate, L = 2,4,6-tris[1-(3-carboxylphenoxy)-ylmethyl]mesitylene, TPT = 2,4,6-tris(4-pyridyl)-1,3,5-triazine, G = guest molecules, BIB = 1,4-bis(imidazol-1-yl)benzene.

5. Conclusions and Future Outlook

Coupling MOFs with various additions to the structures have been shown to enhance the capabilities of the materials with a boost in desired effects. Methods such as covalent attachment, encapsulation, layer-by-layer deposition, in situ formation and MOF templating are effective techniques that can boost materials' intended functions or give rise to new functions in hybrid materials. In addition to enhanced performances, some hybrid materials also benefit from greater stability, increased cyclic use, and reduced cost. For example, some MOF hybrids allow the use of abundant metals instead of precious metals to realize the same type of catalysis with improved outcomes. The synergistic effects of MOF hybrid materials have a vast array of applications that are still expanding. These applications include, but are not limited to, energy harvesting, sensing, catalysis, drug delivery, gas storage, and gas separation.

The increased efficiency of these hybrid materials can open new doors as they are applied to new technologies, but the field is still in its infancy. More research is needed to find ideal material combinations to exploit the strengths of the parent materials, while diminishing their weaknesses. Mechanistic and computational studies are also important to understand how the components interact with each other in the hybrids and investigate what structural features contribute to the enhanced performances. Future work for this field may focus on developing more cost effective synthetic routes as well as increasing efficiency for each hybrid. Discovering new combinations of MOF and other materials may yield better results than existing structures and help to advance the field of material chemistry, as well as reaching new standards for each application.

Funding: This work was funded by American Chemical Society Petroleum Research Fund (grant number: 57951-UNI10), and the National Science Foundation (grant numbers: HRD-1547723 and Amendment 003, DMR-1523588, HRD-1700556).

Conflicts of Interest: The authors declare no conflicts of interest.

References

1. Batten, S.; Champness, N.; Chen, X.-M.; García-Martínez, J.; Kitagawa, S.; Öhrström, L.; O Keeffe, M.; Suh, M.; Reedijk, J. Terminology of metal–organic frameworks and coordination polymers (IUPAC Recommendations 2013)*. *Pure Appl. Chem.* **2013**, *85*, 1715–1724. [CrossRef]
2. Stock, N.; Biswas, S. Synthesis of Metal-Organic Frameworks (MOFs): Routes to Various MOF Topologies, Morphologies, and Composites. *Chem. Rev.* **2012**, *112*, 933–969. [CrossRef] [PubMed]
3. Moghadam, P.Z.; Li, A.; Wiggin, S.B.; Tao, A.; Maloney, A.G.P.; Wood, P.A.; Ward, S.C.; Fairen-Jimenez, D. Development of a Cambridge Structural Database Subset: A Collection of Metal–Organic Frameworks for Past, Present, and Future. *Chem. Mater.* **2017**, *29*, 2618–2625. [CrossRef]
4. Nguyen, J.G.; Cohen, S.M. Moisture-Resistant and Superhydrophobic Metal−Organic Frameworks Obtained via Postsynthetic Modification. *J. Am. Chem. Soc.* **2010**, *132*, 4560–4561. [CrossRef] [PubMed]
5. Yang Seung, J.; Park Chong, R. Preparation of Highly Moisture-Resistant Black-Colored Metal Organic Frameworks. *Adv. Mater.* **2012**, *24*, 4010–4013. [CrossRef] [PubMed]
6. Küsgens, P.; Siegle, S.; Kaskel, S. Crystal Growth of the Metal—Organic Framework Cu3(BTC)2 on the Surface of Pulp Fibers. *Adv. Eng. Mater.* **2009**, *11*, 93–95. [CrossRef]
7. Aijaz, A.; Xu, Q. Catalysis with Metal Nanoparticles Immobilized within the Pores of Metal–Organic Frameworks. *J. Phys. Chem. Lett.* **2014**, *5*, 1400–1411. [CrossRef] [PubMed]
8. Cao, X.; Tan, C.; Sindoro, M.; Zhang, H. Hybrid micro-/nano-structures derived from metal–organic frameworks: Preparation and applications in energy storage and conversion. *Chem. Soc. Rev.* **2017**, *46*, 2660–2677. [CrossRef] [PubMed]
9. Kumar, K.V.; Preuss, K.; Titirici, M.-M.; Rodríguez-Reinoso, F. Nanoporous Materials for the Onboard Storage of Natural Gas. *Chem. Rev.* **2017**, *117*, 1796–1825. [CrossRef] [PubMed]
10. Herm, Z.R.; Bloch, E.D.; Long, J.R. Hydrocarbon Separations in Metal–Organic Frameworks. *Chem. Mater.* **2014**, *26*, 323–338. [CrossRef]

11. Rojas, S.; Carmona, F.J.; Maldonado, C.R.; Horcajada, P.; Hidalgo, T.; Serre, C.; Navarro, J.A.R.; Barea, E. Nanoscaled Zinc Pyrazolate Metal–Organic Frameworks as Drug-Delivery Systems. *Inorg. Chem.* **2016**, *55*, 2650–2663. [CrossRef] [PubMed]
12. Liu, Y.; Howarth Ashlee, J.; Hupp Joseph, T.; Farha Omar, K. Selective Photooxidation of a Mustard-Gas Simulant Catalyzed by a Porphyrinic Metal–Organic Framework. *Angew. Chem. Int. Ed.* **2015**, *54*, 9001–9005. [CrossRef] [PubMed]
13. Li, X.-M.; Dong, L.-Z.; Li, S.-L.; Xu, G.; Liu, J.; Zhang, F.-M.; Lu, L.-S.; Lan, Y.-Q. Synergistic Conductivity Effect in a Proton Sources-Coupled Metal–Organic Framework. *ACS Energy Lett.* **2017**, *2*, 2313–2318. [CrossRef]
14. Huang, W.; Li, S.; Cao, X.; Hou, C.; Zhang, Z.; Feng, J.; Ci, L.; Si, P.; Chi, Q. Metal–Organic Framework Derived Iron Sulfide–Carbon Core–Shell Nanorods as a Conversion-Type Battery Material. *ACS Sustain. Chem. Eng.* **2017**, *5*, 5039–5048. [CrossRef]
15. Buru, C.T.; Li, P.; Mehdi, B.L.; Dohnalkova, A.; Platero-Prats, A.E.; Browning, N.D.; Chapman, K.W.; Hupp, J.T.; Farha, O.K. Adsorption of a Catalytically Accessible Polyoxometalate in a Mesoporous Channel-type Metal–Organic Framework. *Chem. Mater.* **2017**, *29*, 5174–5181. [CrossRef]
16. Chen, Z.; Gu, Z.-G.; Fu, W.-Q.; Wang, F.; Zhang, J. A Confined Fabrication of Perovskite Quantum Dots in Oriented MOF Thin Film. *ACS Appl. Mater. Interfaces* **2016**, *8*, 28737–28742. [CrossRef] [PubMed]
17. He, C.-T.; Tian, J.-Y.; Liu, S.-Y.; Ouyang, G.; Zhang, J.-P.; Chen, X.-M. A porous coordination framework for highly sensitive and selective solid-phase microextraction of non-polar volatile organic compounds. *Chem. Sci.* **2013**, *4*, 351–356. [CrossRef]
18. Wang, Z.; Cohen, S.M. Postsynthetic Covalent Modification of a Neutral Metal−Organic Framework. *J. Am. Chem. Soc.* **2007**, *129*, 12368–12369. [CrossRef] [PubMed]
19. Zhang, W.; Lu, G.; Cui, C.; Liu, Y.; Li, S.; Yan, W.; Xing, C.; Chi Yonggui, R.; Yang, Y.; Huo, F. A Family of Metal-Organic Frameworks Exhibiting Size-Selective Catalysis with Encapsulated Noble-Metal Nanoparticles. *Adv. Mater.* **2014**, *26*, 4056–4060. [CrossRef] [PubMed]
20. Anbia, M.; Hoseini, V. Development of MWCNT@MIL-101 hybrid composite with enhanced adsorption capacity for carbon dioxide. *Chem. Eng. J.* **2012**, *191*, 326–330. [CrossRef]
21. Lu, G.; Farha Omar, K.; Zhang, W.; Huo, F.; Hupp Joseph, T. Engineering ZIF-8 Thin Films for Hybrid MOF-Based Devices. *Adv. Mater.* **2012**, *24*, 3970–3974. [CrossRef] [PubMed]
22. Zhang, R.; Ji, S.; Wang, N.; Wang, L.; Zhang, G.; Li, J.R. Coordination-driven in situ self-assembly strategy for the preparation of metal–organic framework hybrid membranes. *Angew. Chem. Int. Ed.* **2014**, *53*, 9775–9779. [CrossRef] [PubMed]
23. Zou, F.; Hu, X.; Li, Z.; Qie, L.; Hu, C.; Zeng, R.; Jiang, Y.; Huang, Y. MOF-Derived Porous ZnO/$ZnFe_2O_4$/C Octahedra with Hollow Interiors for High-Rate Lithium-Ion Batteries. *Adv. Mater.* **2014**, *26*, 6622–6628. [CrossRef] [PubMed]
24. Guo, W.; Sun, W.; Lv, L.-P.; Kong, S.; Wang, Y. Microwave-Assisted Morphology Evolution of Fe-Based Metal–Organic Frameworks and Their Derived Fe_2O_3 Nanostructures for Li-Ion Storage. *ACS Nano* **2017**, *11*, 4198–4205. [CrossRef] [PubMed]
25. Wang, Z.; Cohen, S.M. Postsynthetic modification of metal–organic frameworks. *Chem. Soc. Rev.* **2009**, *38*, 1315–1329. [CrossRef] [PubMed]
26. Tanabe, K.K.; Cohen, S.M. Postsynthetic modification of metal–organic frameworks—A progress report. *Chem. Soc. Rev.* **2011**, *40*, 498–519. [CrossRef] [PubMed]
27. Choi, J.S.; Bae, J.; Lee, E.J.; Jeong, N.C. A Chemical Role for Trichloromethane: Room-Temperature Removal of Coordinated Solvents from Open Metal Sites in the Copper-Based Metal–Organic Frameworks. *Inorg. Chem.* **2018**, *57*, 5225–5231. [CrossRef] [PubMed]
28. Bae, J.; Choi, J.S.; Hwang, S.; Yun, W.S.; Song, D.; Lee, J.; Jeong, N.C. Multiple Coordination Exchanges for Room-Temperature Activation of Open-Metal Sites in Metal–Organic Frameworks. *ACS Appl. Mater. Interfaces* **2017**, *9*, 24743–24752. [CrossRef] [PubMed]
29. Kim, H.K.; Yun, W.S.; Kim, M.-B.; Kim, J.Y.; Bae, Y.-S.; Lee, J.; Jeong, N.C. A Chemical Route to Activation of Open Metal Sites in the Copper-Based Metal–Organic Framework Materials HKUST-1 and Cu-MOF-2. *J. Am. Chem. Soc.* **2015**, *137*, 10009–10015. [CrossRef] [PubMed]

30. Jeong, N.C.; Samanta, B.; Lee, C.Y.; Farha, O.K.; Hupp, J.T. Coordination-Chemistry Control of Proton Conductivity in the Iconic Metal–Organic Framework Material HKUST-1. *J. Am. Chem. Soc.* **2012**, *134*, 51–54. [CrossRef] [PubMed]
31. Chen, W.; Kuang, Q.; Wang, Q.; Xie, Z. Engineering a High Energy Surface of Anatase TiO_2 Crystals Towards Enhanced Performance for Energy Conversion and Environmental Applications. *RSC Adv.* **2015**, *5*, 20396–20409. [CrossRef]
32. Choi, S.; Watanabe, T.; Bae, T.-H.; Sholl, D.S.; Jones, C.W. Modification of the Mg/DOBDC MOF with Amines to Enhance CO_2 Adsorption from Ultradilute Gases. *J. Phys. Chem. Lett.* **2012**, *3*, 1136–1141. [CrossRef] [PubMed]
33. Li, Z.; Schweitzer, N.M.; League, A.B.; Bernales, V.; Peters, A.W.; Getsoian, A.B.; Wang, T.C.; Miller, J.T.; Vjunov, A.; Fulton, J.L.; et al. Sintering-Resistant Single-Site Nickel Catalyst Supported by Metal–Organic Framework. *J. Am. Chem. Soc.* **2016**, *138*, 1977–1982. [CrossRef] [PubMed]
34. Cui, Y.; Rimoldi, M.; Platero-Prats Ana, E.; Chapman Karena, W.; Hupp Joseph, T.; Farha Omar, K. Stabilizing a Vanadium Oxide Catalyst by Supporting on a Metal–Organic Framework. *ChemCatChem* **2017**, *10*, 1772–1777. [CrossRef]
35. Li, Z.; Peters, A.W.; Liu, J.; Zhang, X.; Schweitzer, N.M.; Hupp, J.T.; Farha, O.K. Size effect of the active sites in UiO-66-supported nickel catalysts synthesized via atomic layer deposition for ethylene hydrogenation. *Inorg. Chem. Front.* **2017**, *4*, 820–824. [CrossRef] [PubMed]
36. Mondloch, J.E.; Bury, W.; Fairen-Jimenez, D.; Kwon, S.; DeMarco, E.J.; Weston, M.H.; Sarjeant, A.A.; Nguyen, S.T.; Stair, P.C.; Snurr, R.Q.; et al. Vapor-Phase Metalation by Atomic Layer Deposition in a Metal–Organic Framework. *J. Am. Chem. Soc.* **2013**, *135*, 10294–10297. [CrossRef] [PubMed]
37. Gallington, L.C.; Kim, I.S.; Liu, W.-G.; Yakovenko, A.A.; Platero-Prats, A.E.; Li, Z.; Wang, T.C.; Hupp, J.T.; Farha, O.K.; Truhlar, D.G.; et al. Regioselective Atomic Layer Deposition in Metal–Organic Frameworks Directed by Dispersion Interactions. *J. Am. Chem. Soc.* **2016**, *138*, 13513–13516. [CrossRef] [PubMed]
38. Kim, I.S.; Borycz, J.; Platero-Prats, A.E.; Tussupbayev, S.; Wang, T.C.; Farha, O.K.; Hupp, J.T.; Gagliardi, L.; Chapman, K.W.; Cramer, C.J.; et al. Targeted Single-Site MOF Node Modification: Trivalent Metal Loading via Atomic Layer Deposition. *Chem. Mater.* **2015**, *27*, 4772–4778. [CrossRef]
39. Peters, A.W.; Li, Z.; Farha, O.K.; Hupp, J.T. Atomically Precise Growth of Catalytically Active Cobalt Sulfide on Flat Surfaces and within a Metal–Organic Framework via Atomic Layer Deposition. *ACS Nano* **2015**, *9*, 8484–8490. [CrossRef] [PubMed]
40. Rimoldi, M.; Bernales, V.; Borycz, J.; Vjunov, A.; Gallington, L.C.; Platero-Prats, A.E.; Kim, I.S.; Fulton, J.L.; Martinson, A.B.F.; Lercher, J.A.; et al. Atomic Layer Deposition in a Metal–Organic Framework: Synthesis, Characterization, and Performance of a Solid Acid. *Chem. Mater.* **2017**, *29*, 1058–1068. [CrossRef]
41. Kung, C.-W.; Mondloch, J.E.; Wang, T.C.; Bury, W.; Hoffeditz, W.; Klahr, B.M.; Klet, R.C.; Pellin, M.J.; Farha, O.K.; Hupp, J.T. Metal–Organic Framework Thin Films as Platforms for Atomic Layer Deposition of Cobalt Ions To Enable Electrocatalytic Water Oxidation. *ACS Appl. Mater. Interfaces* **2015**, *7*, 28223–28230. [CrossRef] [PubMed]
42. Taylor-Pashow, K.M.L.; Della Rocca, J.; Xie, Z.; Tran, S.; Lin, W. Postsynthetic Modifications of Iron-Carboxylate Nanoscale Metal−Organic Frameworks for Imaging and Drug Delivery. *J. Am. Chem. Soc.* **2009**, *131*, 14261–14263. [CrossRef] [PubMed]
43. George, S.M. Atomic Layer Deposition: An Overview. *Chem. Rev.* **2010**, *110*, 111–131. [CrossRef] [PubMed]
44. Fu, J.; Das, S.; Xing, G.; Ben, T.; Valtchev, V.; Qiu, S. Fabrication of COF-MOF Composite Membranes and Their Highly Selective Separation of H_2/CO_2. *J. Am. Chem. Soc.* **2016**, *138*, 7673–7680. [CrossRef] [PubMed]
45. Horcajada, P.; Chalati, T.; Serre, C.; Gillet, B.; Sebrie, C.; Baati, T.; Eubank, J.F.; Heurtaux, D.; Clayette, P.; Kreuz, C.; et al. Porous metal–organic-framework nanoscale carriers as a potential platform for drug delivery and imaging. *Nat. Mater.* **2009**, *9*, 172–178. [CrossRef] [PubMed]
46. Feng, D.; Gu, Z.-Y.; Li, J.-R.; Jiang, H.-L.; Wei, Z.; Zhou, H.-C. Zirconium-Metalloporphyrin PCN-222: Mesoporous Metal–Organic Frameworks with Ultrahigh Stability as Biomimetic Catalysts. *Angew. Chem. Int. Ed.* **2012**, *51*, 10307–10310. [CrossRef] [PubMed]
47. Zhang, F.-M.; Dong, H.; Zhang, X.; Sun, X.-J.; Liu, M.; Yang, D.-D.; Liu, X.; Wei, J.-Z. Postsynthetic Modification of ZIF-90 for Potential Targeted Codelivery of Two Anticancer Drugs. *ACS Appl. Mater. Interfaces* **2017**, *9*, 27332–27337. [CrossRef] [PubMed]

48. Wang, X.-G.; Dong, Z.-Y.; Cheng, H.; Wan, S.-S.; Chen, W.-H.; Zou, M.-Z.; Huo, J.-W.; Deng, H.-X.; Zhang, X.-Z. A multifunctional metal–organic framework based tumor targeting drug delivery system for cancer therapy. *Nanoscale* **2015**, *7*, 16061–16070. [CrossRef] [PubMed]
49. Abánades Lázaro, I.; Haddad, S.; Sacca, S.; Orellana-Tavra, C.; Fairen-Jimenez, D.; Forgan, R.S. Selective Surface PEGylation of UiO-66 Nanoparticles for Enhanced Stability, Cell Uptake, and pH-Responsive Drug Delivery. *Chem* **2017**, *2*, 561–578. [CrossRef] [PubMed]
50. Jahan, M.; Bao, Q.; Loh, K.P. Electrocatalytically Active Graphene–Porphyrin MOF Composite for Oxygen Reduction Reaction. *J. Am. Chem. Soc.* **2012**, *134*, 6707–6713. [CrossRef] [PubMed]
51. Shaikh, N.S.; Enthaler, S.; Junge, K.; Beller, M. Iron-catalyzed enantioselective hydrosilylation of ketones. *Angew. Chem. Int. Ed.* **2008**, *47*, 2497–2501. [CrossRef] [PubMed]
52. Rao, Z.; Feng, K.; Tang, B.; Wu, P. Construction of well interconnected metal-organic framework structure for effectively promoting proton conductivity of proton exchange membrane. *J. Membr. Sci.* **2017**, *533*, 160–170. [CrossRef]
53. Maina, J.W.; Schütz, J.A.; Grundy, L.; Des Ligneris, E.; Yi, Z.; Kong, L.; Pozo-Gonzalo, C.; Ionescu, M.; Dumée, L.F. Inorganic Nanoparticles/Metal Organic Framework Hybrid Membrane Reactors for Efficient Photocatalytic Conversion of CO_2. *ACS Appl. Mater. Interfaces* **2017**, *9*, 35010–35017. [CrossRef] [PubMed]
54. Lu, G.; Li, S.; Guo, Z.; Farha, O.K.; Hauser, B.G.; Qi, X.; Wang, Y.; Wang, X.; Han, S.; Liu, X.; et al. Imparting functionality to a metal-organic framework material by controlled nanoparticle encapsulation. *Nat. Chem.* **2012**, *4*, 310–316. [CrossRef] [PubMed]
55. Zhao, M.; Deng, K.; He, L.; Liu, Y.; Li, G.; Zhao, H.; Tang, Z. Core–Shell Palladium Nanoparticle@Metal–Organic Frameworks as Multifunctional Catalysts for Cascade Reactions. *J. Am. Chem. Soc.* **2014**, *136*, 1738–1741. [CrossRef] [PubMed]
56. Dai, W.; Hu, J.; Zhou, L.; Li, S.; Hu, X.; Huang, H. Removal of Dibenzothiophene with Composite Adsorbent MOF-5/Cu(I). *Energy Fuels* **2013**, *27*, 816–821. [CrossRef]
57. Chen, J.; Wang, S.; Huang, J.; Chen, L.; Ma, L.; Huang, X. Conversion of Cellulose and Cellobiose into Sorbitol Catalyzed by Ruthenium Supported on a Polyoxometalate/Metal–Organic Framework Hybrid. *ChemSusChem* **2013**, *6*, 1545–1555. [CrossRef] [PubMed]
58. Buru, C.T.; Platero-Prats, A.E.; Chica, D.G.; Kanatzidis, M.G.; Chapman, K.W.; Farha, O.K. Thermally induced migration of a polyoxometalate within a metal–organic framework and its catalytic effects. *J. Mater. Chem. A* **2018**, *6*, 7389–7394. [CrossRef]
59. Tang, Y.-J.; Gao, M.-R.; Liu, C.-H.; Li, S.-L.; Jiang, H.-L.; Lan, Y.-Q.; Han, M.; Yu, S.-H. Porous Molybdenum-Based Hybrid Catalysts for Highly Efficient Hydrogen Evolution. *Angew. Chem. Int. Ed.* **2015**, *54*, 12928–12932. [CrossRef] [PubMed]
60. Zou, C.; Zhang, Z.; Xu, X.; Gong, Q.; Li, J.; Wu, C.-D. A Multifunctional Organic–Inorganic Hybrid Structure Based on MnIII–Porphyrin and Polyoxometalate as a Highly Effective Dye Scavenger and Heterogenous Catalyst. *J. Am. Chem. Soc.* **2012**, *134*, 87–90. [CrossRef] [PubMed]
61. Gao, Q.; Xu, S.; Guo, C.; Chen, Y.; Wang, L. Embedding Nanocluster in MOF via Crystalline Ion-Triggered Growth Strategy for Improved Emission and Selective Sensing. *ACS Appl. Mater. Interfaces* **2018**, *10*, 16059–16065. [CrossRef] [PubMed]
62. Drobek, M.; Kim, J.-H.; Bechelany, M.; Vallicari, C.; Julbe, A.; Kim, S.S. MOF-Based Membrane Encapsulated ZnO Nanowires for Enhanced Gas Sensor Selectivity. *ACS Appl. Mater. Interfaces* **2016**, *8*, 8323–8328. [CrossRef] [PubMed]
63. Masih, D.; Chernikova, V.; Shekhah, O.; Eddaoudi, M.; Mohammed, O.F. Zeolite-like Metal–Organic Framework (MOF) Encaged Pt(II)-Porphyrin for Anion-Selective Sensing. *ACS Appl. Mater. Interfaces* **2018**, *10*, 11399–11405. [CrossRef] [PubMed]
64. Lin, X.; Gao, G.; Zheng, L.; Chi, Y.; Chen, G. Encapsulation of Strongly Fluorescent Carbon Quantum Dots in Metal–Organic Frameworks for Enhancing Chemical Sensing. *Anal. Chem.* **2014**, *86*, 1223–1228. [CrossRef] [PubMed]
65. Wang, Z.; Wang, Z.; Lin, B.; Hu, X.; Wei, Y.; Zhang, C.; An, B.; Wang, C.; Lin, W. Warm-White-Light-Emitting Diode Based on a Dye-Loaded Metal–Organic Framework for Fast White-Light Communication. *ACS Appl. Mater. Interfaces* **2017**, *9*, 35253–35259. [CrossRef] [PubMed]

66. Lee, D.Y.; Shin, C.Y.; Yoon, S.J.; Lee, H.Y.; Lee, W.; Shrestha, N.K.; Lee, J.K.; Han, S.-H. Enhanced photovoltaic performance of Cu-based metal-organic frameworks sensitized solar cell by addition of carbon nanotubes. *Sci. Rep.* **2014**, *4*, 3930. [CrossRef] [PubMed]
67. Horiuchi, Y.; Toyao, T.; Saito, M.; Mochizuki, K.; Iwata, M.; Higashimura, H.; Anpo, M.; Matsuoka, M. Visible-Light-Promoted Photocatalytic Hydrogen Production by Using an Amino-Functionalized Ti(IV) Metal–Organic Framework. *J. Phys. Chem. C* **2012**, *116*, 20848–20853. [CrossRef]
68. Agostoni, V.; Horcajada, P.; Noiray, M.; Malanga, M.; Aykaç, A.; Jicsinszky, L.; Vargas-Berenguel, A.; Semiramoth, N.; Daoud-Mahammed, S.; Nicolas, V.; et al. A "green" strategy to construct non-covalent, stable and bioactive coatings on porous MOF nanoparticles. *Sci. Rep.* **2015**, *5*, 7925. [CrossRef] [PubMed]
69. Sun, H.; Tang, B.; Wu, P. Rational Design of S-UiO-66@GO Hybrid Nanosheets for Proton Exchange Membranes with Significantly Enhanced Transport Performance. *ACS Appl. Mater. Interfaces* **2017**, *9*, 26077–26087. [CrossRef] [PubMed]
70. Bae, T.-H.; Lee Jong, S.; Qiu, W.; Koros William, J.; Jones Christopher, W.; Nair, S. A High-Performance Gas-Separation Membrane Containing Submicrometer-Sized Metal–Organic Framework Crystals. *Angew. Chem. Int. Ed.* **2010**, *49*, 9863–9866. [CrossRef] [PubMed]
71. Basu, S.; Cano-Odena, A.; Vankelecom, I.F.J. MOF-containing mixed-matrix membranes for CO_2/CH_4 and CO_2/N_2 binary gas mixture separations. *Sep. Purif. Technol.* **2011**, *81*, 31–40. [CrossRef]
72. Perez, E.V.; Balkus, K.J.; Ferraris, J.P.; Musselman, I.H. Mixed-matrix membranes containing MOF-5 for gas separations. *J. Membr. Sci.* **2009**, *328*, 165–173. [CrossRef]
73. Zhang, Z.; Chen, Y.; He, S.; Zhang, J.; Xu, X.; Yang, Y.; Nosheen, F.; Saleem, F.; He, W.; Wang, X. Hierarchical Zn/Ni-MOF-2 nanosheet-assembled hollow nanocubes for multicomponent catalytic reactions. *Angew. Chem. Int. Ed.* **2014**, *53*, 12517–12521. [CrossRef]
74. Li, R.; Hu, J.; Deng, M.; Wang, H.; Wang, X.; Hu, Y.; Jiang, H.-L.; Jiang, J.; Zhang, Q.; Xie, Y.; et al. Integration of an Inorganic Semiconductor with a Metal–Organic Framework: A Platform for Enhanced Gaseous Photocatalytic Reactions. *Adv. Mater.* **2014**, *26*, 4783–4788. [CrossRef] [PubMed]
75. Lee, D.Y.; Shinde, D.V.; Yoon, S.J.; Cho, K.N.; Lee, W.; Shrestha, N.K.; Han, S.-H. Cu-Based Metal–Organic Frameworks for Photovoltaic Application. *J. Phys. Chem. C* **2014**, *118*, 16328–16334. [CrossRef]
76. Grätzel, M. Conversion of sunlight to electric power by nanocrystalline dye-sensitized solar cells. *J. Photochem. Photobiol. Chem.* **2004**, *164*, 3–14. [CrossRef]
77. Ji, H.; Hwang, S.; Kim, K.; Kim, C.; Jeong, N.C. Direct in Situ Conversion of Metals into Metal–Organic Frameworks: A Strategy for the Rapid Growth of MOF Films on Metal Substrates. *ACS Appl. Mater. Interfaces* **2016**, *8*, 32414–32420. [CrossRef] [PubMed]
78. Lim, J.; Lee, E.J.; Choi, J.S.; Jeong, N.C. Diffusion Control in the in Situ Synthesis of Iconic Metal-Organic Frameworks within an Ionic Polymer Matrix. *ACS Appl. Mater. Interfaces* **2018**, *10*, 3793–3800. [CrossRef] [PubMed]
79. Cui, X.Y.; Gu, Z.Y.; Jiang, D.Q.; Li, Y.; Wang, H.F.; Yan, X.P. In situ hydrothermal growth of metal-organic framework 199 films on stainless steel fibers for solid-phase microextraction of gaseous benzene homologues. *Anal. Chem.* **2009**, *81*, 9771–9777. [CrossRef] [PubMed]
80. Zheng, J.; Li, S.; Wang, Y.; Li, L.; Su, C.; Liu, H.; Zhu, F.; Jiang, R.; Ouyang, G. In situ growth of IRMOF-3 combined with ionic liquids to prepare solid-phase microextraction fibers. *Anal. Chim. Acta* **2014**, *829*, 22–27. [CrossRef] [PubMed]
81. Jeon, J.-W.; Sharma, R.; Meduri, P.; Arey, B.W.; Schaef, H.T.; Lutkenhaus, J.L.; Lemmon, J.P.; Thallapally, P.K.; Nandasiri, M.I.; McGrail, B.P.; et al. In Situ One-Step Synthesis of Hierarchical Nitrogen-Doped Porous Carbon for High-Performance Supercapacitors. *ACS Appl. Mater. Interfaces* **2014**, *6*, 7214–7222. [CrossRef] [PubMed]
82. Chen, C.; Li, B.; Zhou, L.; Xia, Z.; Feng, N.; Ding, J.; Wang, L.; Wan, H.; Guan, G. Synthesis of Hierarchically Structured Hybrid Materials by Controlled Self-Assembly of Metal–Organic Framework with Mesoporous Silica for CO_2 Adsorption. *ACS Appl. Mater. Interfaces* **2017**, *9*, 23060–23071. [CrossRef] [PubMed]
83. Falcaro, P.; Hill, A.J.; Nairn, K.M.; Jasieniak, J.; Mardel, J.I.; Bastow, T.J.; Mayo, S.C.; Gimona, M.; Gomez, D.; Whitfield, H.J.; et al. A new method to position and functionalize metal-organic framework crystals. *Nat. Commun.* **2011**, *2*, 237. [CrossRef] [PubMed]

84. Dybtsev, D.N.; Ponomareva, V.G.; Aliev, S.B.; Chupakhin, A.P.; Gallyamov, M.R.; Moroz, N.K.; Kolesov, B.A.; Kovalenko, K.A.; Shutova, E.S.; Fedin, V.P. High Proton Conductivity and Spectroscopic Investigations of Metal–Organic Framework Materials Impregnated by Strong Acids. *ACS Appl. Mater. Interfaces* **2014**, *6*, 5161–5167. [CrossRef] [PubMed]
85. Chaikittisilp, W.; Hu, M.; Wang, H.; Huang, H.-S.; Fujita, T.; Wu, K.C.W.; Chen, L.-C.; Yamauchi, Y.; Ariga, K. Nanoporous carbons through direct carbonization of a zeolitic imidazolate framework for supercapacitor electrodes. *Chem. Commun.* **2012**, *48*, 7259–7261. [CrossRef] [PubMed]
86. Yang, H.; Kruger, P.E.; Telfer, S.G. Metal–Organic Framework Nanocrystals as Sacrificial Templates for Hollow and Exceptionally Porous Titania and Composite Materials. *Inorg. Chem.* **2015**, *54*, 9483–9490. [CrossRef] [PubMed]
87. Xu, X.; Shi, W.; Li, P.; Ye, S.; Ye, C.; Ye, H.; Lu, T.; Zheng, A.; Zhu, J.; Xu, L.; et al. Facile Fabrication of Three-Dimensional Graphene and Metal–Organic Framework Composites and Their Derivatives for Flexible All-Solid-State Supercapacitors. *Chem. Mater.* **2017**, *29*, 6058–6065. [CrossRef]
88. Malonzo, C.D.; Shaker, S.M.; Ren, L.; Prinslow, S.D.; Platero-Prats, A.E.; Gallington, L.C.; Borycz, J.; Thompson, A.B.; Wang, T.C.; Farha, O.K.; et al. Thermal Stabilization of Metal–Organic Framework-Derived Single-Site Catalytic Clusters through Nanocasting. *J. Am. Chem. Soc.* **2016**, *138*, 2739–2748. [CrossRef] [PubMed]
89. Tan, H.; Ma, C.; Gao, L.; Li, Q.; Song, Y.; Xu, F.; Wang, T.; Wang, L. Metal–Organic Framework-Derived Copper Nanoparticle@Carbon Nanocomposites as Peroxidase Mimics for Colorimetric Sensing of Ascorbic Acid. *Chem. Eur. J.* **2014**, *20*, 16377–16383. [CrossRef] [PubMed]
90. Hwang, Y.K.; Hong, D.-Y.; Chang, J.-S.; Jhung, S.H.; Seo, Y.-K.; Kim, J.; Vimont, A.; Daturi, M.; Serre, C.; Férey, G. Amine Grafting on Coordinatively Unsaturated Metal Centers of MOFs: Consequences for Catalysis and Metal Encapsulation. *Angew. Chem. Int. Ed.* **2008**, *47*, 4144–4148. [CrossRef] [PubMed]
91. Platero-Prats, A.E.; Li, Z.; Gallington, L.C.; Peters, A.W.; Hupp, J.T.; Farha, O.K.; Chapman, K.W. Addressing the characterisation challenge to understand catalysis in MOFs: The case of nanoscale Cu supported in NU-1000. *Faraday Discuss.* **2017**, *201*, 337–350. [CrossRef] [PubMed]
92. Lownsbury, J.M.; Santos-López, I.A.; Zhang, W.; Campbell, C.T.; Yu, H.S.; Liu, W.-G.; Cramer, C.J.; Truhlar, D.G.; Wang, T.; Hupp, J.T.; et al. Calcium Vapor Adsorption on the Metal–Organic Framework NU-1000: Structure and Energetics. *J. Phys. Chem. C* **2016**, *120*, 16850–16862. [CrossRef]
93. Rimoldi, M.; Gallington Leighanne, C.; Chapman Karena, W.; MacRenaris, K.; Hupp Joseph, T.; Farha Omar, K. Catalytically Active Silicon Oxide Nanoclusters Stabilized in a Metal–Organic Framework. *Chem. Eur. J.* **2017**, *23*, 8532–8536. [CrossRef] [PubMed]
94. Beyzavi, M.H.; Klet, R.C.; Tussupbayev, S.; Borycz, J.; Vermeulen, N.A.; Cramer, C.J.; Stoddart, J.F.; Hupp, J.T.; Farha, O.K. A Hafnium-Based Metal–Organic Framework as an Efficient and Multifunctional Catalyst for Facile CO_2 Fixation and Regioselective and Enantioretentive Epoxide Activation. *J. Am. Chem. Soc.* **2014**, *136*, 15861–15864. [CrossRef] [PubMed]
95. Kim, I.S.; Li, Z.; Zheng, J.; Platero-Prats Ana, E.; Mavrandonakis, A.; Pellizzeri, S.; Ferrandon, M.; Vjunov, A.; Gallington Leighanne, C.; Webber Thomas, E.; et al. Sinter-Resistant Platinum Catalyst Supported by Metal–Organic Framework. *Angew. Chem. Int. Ed.* **2017**, *57*, 909–913. [CrossRef] [PubMed]
96. Ahn, S.; Nauert, S.L.; Buru, C.T.; Rimoldi, M.; Choi, H.; Schweitzer, N.M.; Hupp, J.T.; Farha, O.K.; Notestein, J.M. Pushing the Limits on Metal–Organic Frameworks as a Catalyst Support: NU-1000 Supported Tungsten Catalysts for o-Xylene Isomerization and Disproportionation. *J. Am. Chem. Soc.* **2018**, *140*, 8535–8543. [CrossRef] [PubMed]
97. Tanabe, K.K.; Cohen, S.M. Engineering a metal-organic framework catalyst by using postsynthetic modification. *Angew. Chem. Int. Ed.* **2009**, *48*, 7424–7427. [CrossRef] [PubMed]
98. Toyao, T.; Miyahara, K.; Fujiwaki, M.; Kim, T.-H.; Dohshi, S.; Horiuchi, Y.; Matsuoka, M. Immobilization of Cu Complex into Zr-Based MOF with Bipyridine Units for Heterogeneous Selective Oxidation. *J. Phys. Chem. C* **2015**, *119*, 8131–8137. [CrossRef]
99. Ingleson, M.J.; Barrio, J.P.; Guilbaud, J.B.; Khimyak, Y.Z.; Rosseinsky, M.J. Framework functionalisation triggers metal complex binding. *Chem. Commun.* **2008**, *23*, 2680–2682. [CrossRef] [PubMed]

100. Deng, X.; Albero, J.; Xu, L.; García, H.; Li, Z. Construction of a Stable Ru–Re Hybrid System Based on Multifunctional MOF-253 for Efficient Photocatalytic CO_2 Reduction. *Inorg. Chem.* **2018**, *57*, 8276–8286. [CrossRef] [PubMed]
101. Chen, L.; Chen, H.; Li, Y. One-pot synthesis of Pd@MOF composites without the addition of stabilizing agents. *Chem. Commun.* **2014**, *50*, 14752–14755. [CrossRef] [PubMed]
102. Han, Q.; He, C.; Zhao, M.; Qi, B.; Niu, J.; Duan, C. Engineering Chiral Polyoxometalate Hybrid Metal–Organic Frameworks for Asymmetric Dihydroxylation of Olefins. *J. Am. Chem. Soc.* **2013**, *135*, 10186–10189. [CrossRef] [PubMed]
103. Kaur, R.; Sharma, A.L.; Kim, K.-H.; Deep, A. A novel CdTe/Eu-MOF photoanode for application in quantum dot-sensitized solar cell to improve power conversion efficiency. *J. Ind. Eng. Chem.* **2017**, *53*, 77–81. [CrossRef]
104. Liu, J.-J.; Shan, Y.-B.; Fan, C.-R.; Lin, M.-J.; Huang, C.-C.; Dai, W.-X. Encapsulating Naphthalene in an Electron-Deficient MOF to Enhance Fluorescence for Organic Amines Sensing. *Inorg. Chem.* **2016**, *55*, 3680–3684. [CrossRef] [PubMed]
105. Huang, W.; Pan, F.; Liu, Y.; Huang, S.; Li, Y.; Yong, J.; Li, Y.; Kirillov, A.M.; Wu, D. An Efficient Blue-Emissive Metal–Organic Framework (MOF) for Lanthanide-Encapsulated Multicolor and Stimuli-Responsive Luminescence. *Inorg. Chem.* **2017**, *56*, 6362–6370. [CrossRef] [PubMed]
106. Jahan, M.; Liu, Z.; Loh, K.P. A Graphene Oxide and Copper-Centered Metal Organic Framework Composite as a Tri-Functional Catalyst for HER, OER, and ORR. *Adv. Funct. Mater.* **2013**, *23*, 5363–5372. [CrossRef]
107. Yang, S.J.; Hyun Cho, J.; Nahm, K.-S.; Park, C. Enhanced hydrogen storage capacity of Pt-loaded CNT@MOF-5 hybrid composites. *Int. J. Hydrog. Energy* **2010**, *35*, 13062–13067. [CrossRef]
108. Jiang, H.; Feng, Y.; Chen, M.; Wang, Y. Synthesis and hydrogen-storage performance of interpenetrated MOF-5/MWCNTs hybrid composite with high mesoporosity. *Int. J. Hydrog. Energy* **2013**, *38*, 10950–10955. [CrossRef]
109. Yang, S.J.; Choi, J.Y.; Chae, H.K.; Cho, J.H.; Nahm, K.S.; Park, C.R. Preparation and Enhanced Hydrostability and Hydrogen Storage Capacity of CNT@MOF-5 Hybrid Composite. *Chem. Mater.* **2009**, *21*, 1893–1897. [CrossRef]
110. Zhou, H.; Liu, X.; Zhang, J.; Yan, X.; Liu, Y.; Yuan, A. Enhanced room-temperature hydrogen storage capacity in Pt-loaded graphene oxide/HKUST-1 composites. *Int. J. Hydrog. Energy* **2014**, *39*, 2160–2167. [CrossRef]
111. Xiang, Z.; Hu, Z.; Cao, D.; Yang, W.; Lu, J.; Han, B.; Wang, W. Metal–Organic Frameworks with Incorporated Carbon Nanotubes: Improving Carbon Dioxide and Methane Storage Capacities by Lithium Doping. *Angew. Chem. Int. Ed.* **2010**, *50*, 491–494. [CrossRef] [PubMed]
112. Song, Z.; Qiu, F.; Zaia, E.W.; Wang, Z.; Kunz, M.; Guo, J.; Brady, M.; Mi, B.; Urban, J.J. Dual-Channel, Molecular-Sieving Core/Shell ZIF@MOF Architectures as Engineered Fillers in Hybrid Membranes for Highly Selective CO_2 Separation. *Nano Lett.* **2017**, *17*, 6752–6758. [CrossRef] [PubMed]
113. Yang, Y.; Lun, Z.; Xia, G.; Zheng, F.; He, M.; Chen, Q. Non-precious alloy encapsulated in nitrogen-doped graphene layers derived from MOFs as an active and durable hydrogen evolution reaction catalyst. *Energy Environ. Sci.* **2015**, *8*, 3563–3571. [CrossRef]
114. Liu, B.; Shioyama, H.; Akita, T.; Xu, Q. Metal-Organic Framework as a Template for Porous Carbon Synthesis. *J. Am. Chem. Soc.* **2008**, *130*, 5390–5391. [CrossRef] [PubMed]
115. Bai, X.; Liu, Q.; Lu, Z.; Liu, J.; Chen, R.; Li, R.; Song, D.; Jing, X.; Liu, P.; Wang, J. Rational Design of Sandwiched Ni–Co Layered Double Hydroxides Hollow Nanocages/Graphene Derived from Metal–Organic Framework for Sustainable Energy Storage. *ACS Sustain. Chem. Eng.* **2017**, *5*, 9923–9934. [CrossRef]
116. Zhang, Y.; Lin, B.; Sun, Y.; Han, P.; Wang, J.; Ding, X.; Zhang, X.; Yang, H. MoO_2@Cu@C Composites Prepared by Using Polyoxometalates@Metal-Organic Frameworks as Template for All-Solid-State Flexible Supercapacitor. *Electrochim. Acta* **2016**, *188*, 490–498. [CrossRef]
117. Shen, J.Q.; Liao, P.Q.; Zhou, D.D.; He, C.T.; Wu, J.X.; Zhang, W.X.; Zhang, J.P.; Chen, X.M. Modular and Stepwise Synthesis of a Hybrid Metal-Organic Framework for Efficient Electrocatalytic Oxygen Evolution. *J. Am. Chem. Soc.* **2017**, *139*, 1778–1781. [CrossRef] [PubMed]
118. Ma, T.Y.; Dai, S.; Jaroniec, M.; Qiao, S.Z. Metal–organic framework derived hybrid Co_3O_4-carbon porous nanowire arrays as reversible oxygen evolution electrodes. *J. Am. Chem. Soc.* **2014**, *136*, 13925–13931. [CrossRef] [PubMed]

119. Tian, D.; Zhou, X.-L.; Zhang, Y.-H.; Zhou, Z.; Bu, X.-H. MOF-Derived Porous Co_3O_4 Hollow Tetrahedra with Excellent Performance as Anode Materials for Lithium-Ion Batteries. *Inorg. Chem.* **2015**, *54*, 8159–8161. [CrossRef] [PubMed]
120. Zhou, X.; Chen, S.; Yang, J.; Bai, T.; Ren, Y.; Tian, H. Metal–Organic Frameworks Derived Okra-like SnO_2 Encapsulated in Nitrogen-Doped Graphene for Lithium Ion Battery. *ACS Appl. Mater. Interfaces* **2017**, *9*, 14309–14318. [CrossRef] [PubMed]
121. Zou, K.-Y.; Liu, Y.-C.; Jiang, Y.-F.; Yu, C.-Y.; Yue, M.-L.; Li, Z.-X. Benzoate Acid-Dependent Lattice Dimension of Co-MOFs and MOF-Derived CoS2@CNTs with Tunable Pore Diameters for Supercapacitors. *Inorg. Chem.* **2017**, *56*, 6184–6196. [CrossRef] [PubMed]